

ROLE OF VISCOSITY IN HYPERSONIC INTAKE STARTING PHENOMENON

Soumyajit Saha; Debasis Chakraborty
 Directorate of Computational Dynamics
 Defence Research and Development Laboratory (DRDL)
 Kanchanbagh Post, Hyderabad-500 058
 Email : debasis_cfd@drdl.drdo.in; debasis_drld@yahoo.co.in

Abstract

Starting and unstarting characteristics of a hypersonic air intake is studied through inviscid and viscous simulations. Comparison of simulated center body Mach number obtained from Euler simulations for different free stream Mach numbers show a much crisper solution for the present computation as compared to other simulations reported in the literature. For Euler simulation, hysteresis effect of intake pressure recovery and mass capture ratio were observed. The hysteresis of pressure recovery clearly showed distinct point of starting / unstarting of the intake. The same hysteresis effect could not be observed for viscous simulation. Well resolved viscous simulations are required for estimation of hypersonic intake characteristics.

Introduction

The performance of a ramjet/scramjet powered hypersonic vehicle is determined by its intake efficiency as the engine performance depends very much on the quantity and quality (non-uniformity and total pressure) of the flow entering the engine. The design criteria of air intake are well documented in the literature [1]. The intake should provide adequate mass flow of air as demanded by the combustor and compress the flow as efficiently as possible minimizing viscous and shock losses. Intake must be able to tolerate the back pressure caused by heat addition and its performance should not be significantly reduced by operation at incidence. The velocity profile at intake exit should be as uniform as possible and drag due to intake should be kept at minimum. Small loss in intake efficiency translates to a substantial penalty in engine thrust. Therefore the detailed analysis and assessment of flow behavior through the intake and its interaction with external flow play an important role in design evaluation and system performance optimization.

Mixed compression intakes which are combination of internal and external compression are generally employed in hypersonic vehicles. The schematic flow pattern in mixed compression intake is shown in Fig.1. Free stream flow after encountering bow shock of vehicle forebody

undergoes number of compression at the central body which coalesces at the cowl lip at design Mach number. The cowl geometry turns the flow inward to the axial direction. The forebody boundary layer after interaction with the centerbody and cowl shocks may separate. Despite simple geometry, the intake is very sensitive to upstream external flow and downstream combustion process and exhibits complex flow phenomena over its range of operation.

Mixed compression hypersonic intakes often possess "unstart problem". For scramjet operation, the freestream Mach number is reduced by a factor of about 3 before it enters the combustor. Such highly convergent duct can support two different flow configurations, namely; (1) A bow shock in front of the intake that spills some flow and the intake flow is subsonic ('unstarted') (2) no bow shock, no spillage and flow is supersonic throughout ('started flow'). Over-contraction, variation of flight conditions, increase of back pressure in combustor or combined effect of these factors can cause intake to unstart. Kantrowitz correlation (theoretical maximum permissible ratio of area at entry to that at the throat (A/A^*)) is defined [2] based on the theory of oblique shocks for starting of an internal compression intake. This however does not hold for hypersonic intakes where the interaction of boundary layer with internal shocks are conjectured to be the prime cause

of flow separation leading to oscillatory flow structure and expulsion of the shock causing unstart of the intake. 'Started' flow condition is required for scramjet operation. Under steady flow freestream conditions, high contraction ratio intakes do not start spontaneously. The normal shock, in front of the unstarted intake needs to be swallowed for the establishment of stable supersonic flow in the intake. Various method namely (1) variable intake geometry, (2) bleed bypass (3) overboard spillage and (4) starting using unsteady effects etc. are proposed in the literature [3-4] to start hypersonic intakes at any flight condition. For high speed flows ($M_\infty \sim 6$), with high total temperature (~ 1800 K), any complex mechanical control system may cause severe structural and cooling problems. The predictions of intake unstart and the mitigation plan to reduce its occurrence is very much essential for hypersonic intake design.

Both numerical and experimental research [5-7] is in progress to understand the causes of hypersonic intake unstart and means to avoid it. Schneider and Koschel [8] carried out experimental and numerical studies of starting and throttling behavior of 9 different intake configurations and shown that separation bubble size at ramp surface depend largely on geometry selection. The role of internal contraction ratios and different bleed dimensions on starting characteristics of 2D and 3D hypersonic intakes was studied experimentally by Haberle and Gulhan [9,10]. Das and Prasad [11] have shown that small angle at the cowl lip leads to start of the intake and improve the performance of mixed compression intake flow field at Mach 2.2 with different cowl deflections. The interaction of forebody shock and cowl lip shock was studied by Lind et al. [12] and predicted very high pressure and temperature region around the cowl lip resulting in flow instability in the intake. Brenneis et al. [13] observed drastic change in flowfield behavior of 2-D inlet at $M=7.4$ with adiabatic wall compared to fixed temperature wall. Saha and Chakraborty [14] also found pronounced effect of adiabatic / isothermal wall boundary condition on starting Mach number for hypersonic intake with side fencing. Heated boundary layer for adiabatic condition is seen to cause large separation bubble at the intake entrance causing flow unstarting; while flow separation bubble is not observed for isothermal condition for same free stream Mach number. Donde et al. [15] carried out numerical simulation of starting problem in a variable geometry hypersonic intake with a movable cowl. It was shown that the cowl needs to be rotated through 15.7° and then be brought back to the original position for restarting of the intake after an 'un-

start'. It is clear from the above discussion that the starting problem of hypersonic intake is not fully understood and the flow field inside the air intake need to be investigated accurately to tackle this undesirable phenomenon.

For any numerical simulation in design exercise, validation is one of the most important activities, where known results are reproduced to obtain the error band and range of application of the software. Keeping that goal in mind, commercial CFD software is applied, in the present study, to a typical hypersonic air intake [16] configuration at different freestream Mach numbers to numerically explore its starting/unstarting behavior. Computed flow field is compared with other numerical results and the role of viscosity in the prediction of starting characteristics is investigated.

Computational Details

Figure 2 shows the intake geometry with length and height are nondimensionalised with throat height ($h=0.01$ m). The 2D computational domain was discretised by 40 thousand nodes (160×250 nodes in flow and intake height directions) using ICEMCFD mesh generator. Fig.3a shows the grid in the whole domain, along with boundary conditions. Zoomed view of grid at cowl region is shown in Fig.3b. The domain shape is chosen such a way that the external shock system is contained within the computational domain and the reflection of the shock from the outer boundary does not influence the solution. The angles of the domain are so determined that all characteristics lines enter the domain from inlet and leave the domain from outlet. Pressure inlet condition was prescribed for ambient condition, with total temperature of 300K. Total pressure was varied for simulation of different Mach numbers with a constant static pressure of 1bar. Ambient outlet was prescribed as pressure outlet of 1bar, and intake outlet was prescribed 0.1 bar pressure which is low enough to ensure a supersonic flow. For RANS (Reynolds Averaged Navier Stokes) simulations, adiabatic and no slip wall conditions are considered for the intake walls. Both Euler and RANS (with SST- $k\omega$ turbulence model) simulations were carried out to study the starting and unstarting characteristics of the air intake using commercial CFD software Fluent [17]. Second order spatial accurate Roe-FDS (Finite Difference Scheme) was used for flux estimation. Three decades fall of maximum residue is considered as convergence criteria.

Results and Discussions

Simulation with Euler Solver

Simulation was first carried out for freestream Mach number of 4.5. The converged solution showed a started intake with shock on lip. The features of the flow field are shown in Fig.4 by depicting the Mach number distribution in the symmetry plane. The flow is supersonic throughout and shock reflections in the intake are captured crisply. The axial distribution of centerbody Mach number is compared with two different inviscid solutions(CFL3D [18] and UTNS [19]) in Fig.5. The difference of Mach number is clearly seen first on the ramp surface ($X \sim [5-12\text{cm}]$). Oblique shock relations show a value of post shock Mach number 2.97 on 18° ramp surface for freestream Mach number 4.5. The present simulation predicts the Mach number close to the oblique relation; whereas the other two solvers show a much lower Mach number of about 2.5. The shock reflections inside the intake in literature value [16] are not as crisp as the present simulation.

Simulations were carried out for a decreasing sequence of inlet Mach number of 3.5, 3, 2.8, 2.7, 2.6, each time starting from the started solution of the previous higher freestream Mach number. It was observed that the intake remains started as the freestream Mach number reduced till 2.6 from 4.5. As the inlet Mach number is reduced further to 2.5 from a started intake at 2.6, the converged solution shows an unstarted condition of the intake at Mach 2.5. Fig.6 compares the axial distribution of Mach number on centerbody with the two literature reported simulation data for Mach 3. Present simulation crisply picked up the shock structure in the started intake. Flow features of the unstarted intake at Mach 2.5 is presented in the Mach number contour plot in Fig.7. A normal shock stands clearly ahead of the cowl lip. The centerbody Mach number is plotted along with CFD results of the other two literature reported simulations in Fig.8 for freestream Mach 2.5. The Mach number falls below $M=1$ from a supersonic flow representing a normal shock. A small decrease in freestream flow results in a drastic change of flow field in the intake as seen in the Mach number distributions presented in Figs.9a and 9b for free stream Mach number 2.6 and 2.5 respectively.

Once unstarted, the inlet freestream Mach number was increased in steps till 3.3. The intake remains unstarted as freestream Mach number is increased from 2.5 to 3.3. When freestream Mach was further increased from 3.3 to 3.4, the intake showed a started flow condition. The starting of the air intake as freestream Mach number is in-

creased from Mach 3.3 to Mach 3.4 is shown in Figs.10a and 10b respectively.

Intake Performance and Hysteresis Effect

Figure 11 plots total pressure recovery at intake exit for different freestream Mach numbers. The red curve shows the increase of total pressure recovery for the started intake, as the freestream inlet Mach number is decreased from 4.5 to 2.6. The intake remains started till freestream Mach 2.6 below which it unstarts and the total pressure (p_0) drops sharply. Similarly total pressure decreases for an unstarted intake with increased inlet Mach number till 3.3, above which the total pressure increases to a value corresponding to a started intake. The sharp variation in total pressure recovery at both start and unstart of intake, makes the parameter a good choice for detecting the starting and unstarting of intakes. The hysteresis behaviour of intake is also presented in the mass capture ratio vs. Mach number plot in Fig.12. It can be seen that the change of mass capture ratio at unstart and starting of intake is not as significant as the corresponding changes in total pressure recovery.

Simulation with RANS Solver

Simulations are also carried out to test unstarting and starting of the intake using RANS solver with SST- $k\omega$ turbulence model using Fluent software. The pressure comparison for cowl and centerbody surfaces between Euler and RANS simulation for free stream Mach number 2.5 is shown in Fig.13. Although surface pressures for this unstarting conditions are not vastly different, the flow characteristics between inviscid and viscous cases differ very much for intake operation. Fig.14 plots the total pressure recovery vs. freestream Mach number for the intake operation. The red curve shows the unstarting of intake from a started condition by reducing freestream Mach number. The blue curve shows the starting of intake from unstarted condition by increasing the freestream Mach number. Unlike the Euler simulations, the RANS simulations do not show any distinct variation of total pressure showing the point of intake unstarting or starting. Figs.15a and 15b show the flow field as the intake gets unstarted from a started intake at Mach 3.0 to an unstarted Mach 2.5 respectively. To get an unstarted flow field, the inlet Mach number had to be changed significantly (from Mach 3.0 to Mach 2.5). As the intake starts from a Mach 4.3 to Mach 4.5 (as inferred from the total pressure recovery vs. Mach number curve of Fig.12), there is no signifi-

cant variation in flow as can be seen in Figs.16a and 16b corresponding to the two Mach numbers.

Conclusions

Both Euler and RANS solvers with SST- $k\omega$ turbulence model were used to numerically investigate unstarting and starting of a 2D intake. Computed centerbody Mach number for different freestream Mach numbers compares very well to other Euler simulation results reported in literature. In fact, the present simulation capture flow field much crisper compared to the other numerical results and predicted surface Mach number matches well with the oblique shock relation. For Euler simulation, there is distinct hysteresis effect and pressure recovery shows a distinct point of starting/unstarting location. The same hysteresis effect could not be observed for viscous simulation and starting/unstarting Mach number of the intake is vastly different compared to its inviscid counterpart. Present computations clearly brings out that inviscid simulation is inadequate and well resolved viscous simulation is required to capture starting/unstarting characteristics of hypersonic intakes.

References

1. Seddon, J. and Goldsmith, E.L., "Intake Aerodynamics", AIAA Education Series, 1985.
2. Kantrowitz A. and Donaldson, C., "Preliminary Investigation of Supersonic Diffusers", NACA WR L-713, 1945.
3. Dirk, S., Andreas, H. and Ulrich, W., "Reduction of Shock Induced Boundary Layer Separation In Hypersonic Inlets Using Bleed", Aerospace Science and Technology, Vol.2, Issue 4, 1998, pp.231-239.
4. Molder. S., Timofeev, E.V. and Tahir, R. B., "Flow Starting in High Compression Hypersonic Air Inlets by Mass Spillage", AIAA Paper No.2004-4130, 2004.
5. Donde, P., Marathe, A. G. and Sudhakar, K., "Starting in Hypersonic Intakes", AIAA Paper No. 2006-4510.
6. Lu, P. J. and Jain, L.T., "Numerical Investigation of Inlet Buzz Flow", AIAA Journal, Vol.14, No.1, 1998, pp.90-100.
7. Oh, J. Y., Fuhara Ma., Shih-Yang Hseih and Vigor Yang., "Interactions Between Shock and Acoustic Waves in a Supersonic Inlet Diffuser", Journal of Propulsion and Power, Vol. 21, No.3, 2005, pp.486-494.
8. Schneider, A. and Koschel, W.W., "Detailed Analysis of a Mixed Compression Hypersonic Intake", ISABE Paper No.99-7036, 1999.
9. Haberle, J. and Gulhan, A., "Experimental Investigation of a Two-Dimensional and Three Dimensional Scramjet Inlet at Mach 7", Journal of Propulsion and Power, Vol. 24, No.5, October 2008, pp.1023-1034.
10. Haberle, J. and Gulhan, A., "Internal Flowfield Investigation of Hypersonic Inlet at Mach 6 with Bleed", Journal of Propulsion and Power, Vol.23, No.5 2007, pp.1007-1017.
11. Das, S. and Prasad, J. K., "Starting Characteristics of a Rectangular Supersonic Airintake with Cowl Deflection", The Aeronautical Journal, Vol.114, No.3, March 2010, pp.177-189.
12. Lind, C. A. and Lewis, M. J., "The Effect of Shock/Shock Interactions on the Design of Hypersonic Inlets", AIAA Paper No. 90-2217, 1990.
13. Brenneis, A. and Wanie, K. M., "Navier-Stokes Results for Hypersonic Inlet Flows", AIAA Paper No.91-2472, 1991.
14. Soumyajit Saha and Debasis Chakraborty., "Hypersonic Intake Starting Characteristics - A CFD Validation Study", Defence Science Journal, Vol. 62, No.3, May 2012, pp.147-152.
15. Donde, P., Marathe, A. G. and Sudhakar, K., "Starting in Hypersonic Intakes", AIAA Paper No.2006-4510.
16. Barber, T. J., David, H. and Fastenberg, S., "CFD Modeling of Hypersonic Inlet Starting Problem", AIAA 2006-123, January 2006.
17. Ansys Fluent User Guide Release 14.0 Ansys Inc. November 2011.

18. Choi, D., "Three-Dimensional Navier-Stokes Analysis for a Tip Leakage Flow in a Low Aspect Ratio Turbine", AIAA 92-0395, January 1992.

19. Rumsey, C. and Anderson, W., "Some Numerical and Physical Aspects of Unsteady Navier-Stokes Computations Over Airfoils Using Dynamic Meshes", AIAA 88-0329, January 1988.

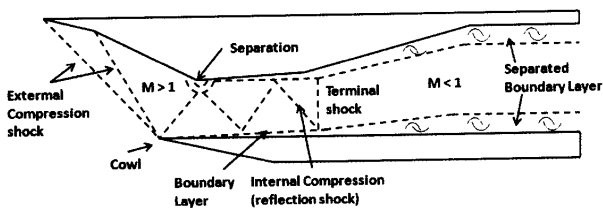


Fig.1 Schematic of the Flow Field in Mixed Compression Intake

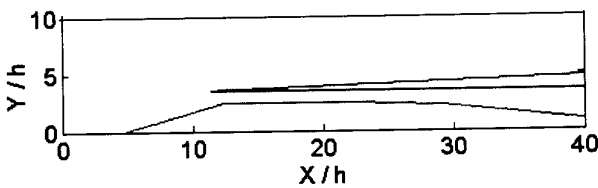


Fig.2 Intake Geometry (Nondimensionalised with Throat Height)

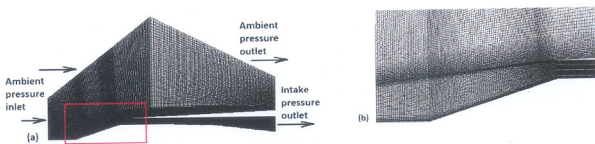


Fig.3 Computational Domain and Grid Showing Boundaries for Air Intake

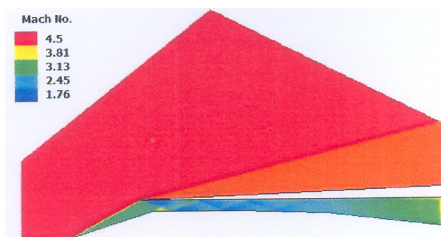


Fig.4 Mach Number Contour of Started Intake for $M_\infty = 4.5$

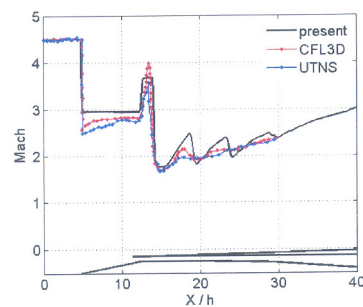


Fig.5 Axial Distribution of Mach Number on Center Body for $M_\infty = 4.5$

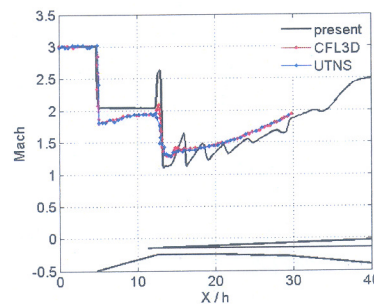


Fig.6 Axial Distribution of Mach Number on Center Body for $M_\infty = 3.0$

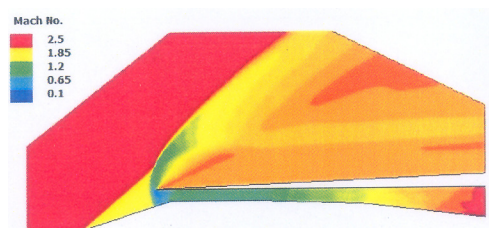


Fig.7 Mach Number Contour of Unstarted Intake for $M_\infty = 2.5$

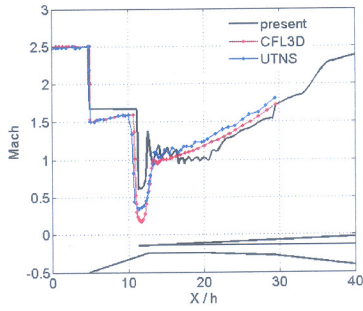


Fig.8 Axial Distribution of Mach Number on Center Body for $M_\infty = 2.5$

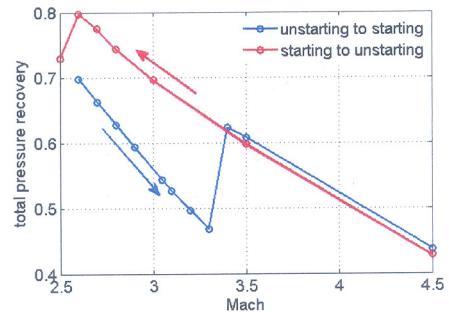


Fig.11 Total Pressure Recovery Vs. Freestream Inlet Mach Number for Euler Simulations

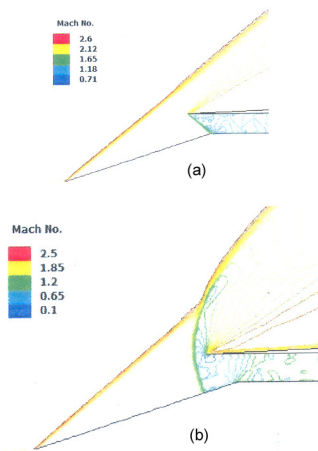


Fig.9 Mach Number Contour for (a) $M_\infty = 2.6$ Just Before Unstart, and (b) $M_\infty = 2.5$ After Unstart

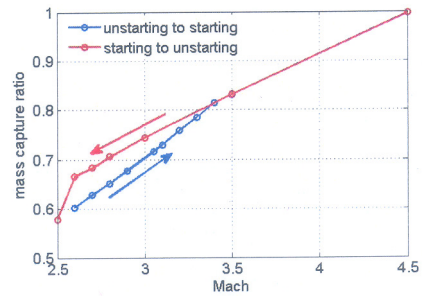


Fig.12 Mass Capture Ratio Vs. Freestream Inlet Mach Number

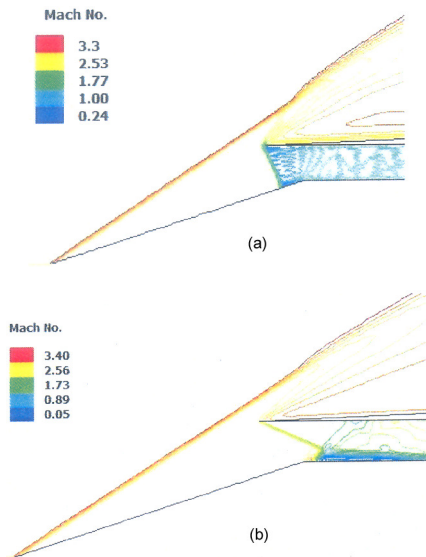


Fig.10 Mach Number Contour for (a) $M_\infty = 3.3$ Just Before Starting, and (b) $M_\infty = 3.4$ After Starting

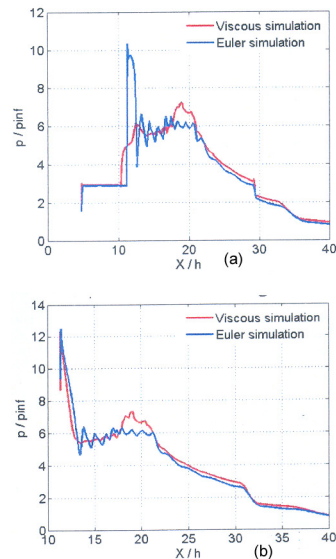


Fig.13 Pressure Comparison for (a) Centerbody and (b) Cowl Surfaces for $M_\infty = 2.5$

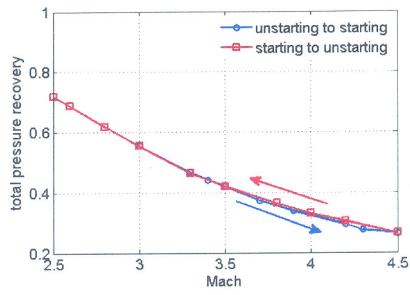


Fig.14 Total Pressure Recovery Vs. Freestream Mach Number for RANS Simulations

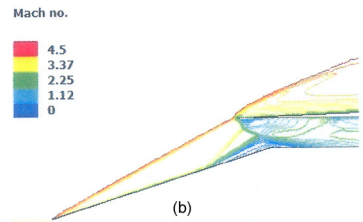
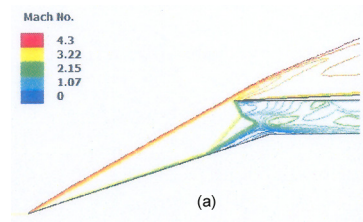


Fig.16 Mach Number Contour for (a) $M_\infty = 4.3$ Before Starting, and (b) $M_\infty = 4.5$ After Starting

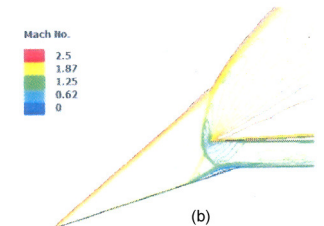
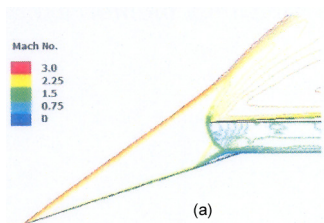


Fig.15 Mach Number Contour for (a) $M_\infty = 3.0$ Before Unstart, and (b) $M_\infty = 2.5$ After Unstart